



# OPEN Obesity exacerbates experimental colitis due to the activation of the local renin–angiotensin system in the colon

Maomao Pan<sup>1</sup>, Qiang Xu<sup>1</sup>, Linjing Huang<sup>1</sup>, Yuanyuan Bai<sup>2</sup>, Xue Li<sup>3,4</sup>✉ & Yibing Tang<sup>1</sup>✉

Obesity is recognized as a risk factor for inflammatory bowel disease (IBD) and may contribute to its progression. However, the underlying mechanisms remain unclear. This study aimed to investigate the impact of high-fat diet (HFD)-induced obesity on the development of experimental colitis, with a particular focus on the role of the gut renin–angiotensin system (RAS) in this process. C57BL/6J mice were assigned to either a low-fat diet (LFD) or HFD for 10 weeks to establish an obesity model. The severity of colitis was significantly greater in obese mice compared to those fed the LFD. Additionally, obesity was associated with increased levels of IL-6, IFN- $\gamma$ , and TNF- $\alpha$ , while simultaneously downregulating the expression of occludin proteins in the colon, leading to increased colonic permeability in the obese mice. Following colitis induction, HFD-induced obesity activated the RAS by upregulating the expression of angiotensin II receptor, angiotensinogen, and renin in the colon. Treatment with a RAS inhibitor significantly alleviated the symptoms of colitis in the obese mice. These findings suggest that HFD-induced obesity enhances intestinal mucosal barrier permeability and exacerbates mucosal inflammation through the activation of the local RAS, thereby promoting colitis.

**Keywords** Inflammatory bowel disease (IBD), Obesity, Renin–angiotensin system (RAS), Intestinal epithelial barrier

Inflammatory bowel disease (IBD) is a complex disorder characterized by chronic inflammation of the gastrointestinal tract, with two primary clinical subtypes: Crohn's disease (CD) and Ulcerative colitis (UC). The incidence of IBD is thought to be associated with factors such as industrialization, changes in living conditions, and dietary practices, contributing to its global spread<sup>1</sup>. The etiology of IBD remains incompletely understood but is believed to involve dysregulation of the mucosal immune response by the gut microbiota and impairment of the intestinal barrier, with numerous pro-inflammatory mediators playing a role<sup>2</sup>. The intestinal barrier system comprises a mucus layer, intestinal epithelial cells (IECs), tight junctions (TJs), immune cells, and gut microbiota, all of which can be influenced by external factors such as dietary fats<sup>3,4</sup>. Multiple studies have suggested a potential link between the pathogenesis of IBD and Western diets, which are characterized by high levels of saturated fat, sugar, and insufficient fiber<sup>5–7</sup>. Moreover, evidence indicates that obesity resulting from a high-fat diet could contribute to the development of IBD<sup>8,9</sup>.

Obesity is a chronic metabolic disorder that has seen a dramatic rise in global prevalence over the past five decades, reaching epidemic proportions and posing a major health risk worldwide<sup>10</sup>. Obesity is increasingly recognized as a chronic low-grade inflammatory state, with adipose tissue playing a key role in the regulation of inflammation. Research has shown a significant correlation between obesity, intestinal inflammation, and dysfunction of the intestinal barrier<sup>11–14</sup>, suggesting that obesity may be a potential risk factor for IBD. A prominent feature observed in individuals with obesity and related conditions is the high prevalence of a leaky or hyper-permeable gut<sup>15</sup>. Additionally, all components of the renin–angiotensin system (RAS) are present

<sup>1</sup>Department of Pathology, The Second Affiliated Hospital and Yuying Children's Hospital of Wenzhou Medical University, Wenzhou 325000, Zhejiang, China. <sup>2</sup>Department of Clinical Laboratory, The Second Affiliated Hospital and Yuying Children's Hospital of Wenzhou Medical University, Wenzhou 325000, Zhejiang, China. <sup>3</sup>Urology & Nephrology Center, Department of Urology, Zhejiang Provincial People's Hospital (Affiliated People's Hospital), Hangzhou Medical College, Hangzhou 310013, Zhejiang, China. <sup>4</sup>Clinical Medicine Research Institute, Zhejiang Provincial People's Hospital (Affiliated People's Hospital), Hangzhou Medical College, Hangzhou 310013, Zhejiang, China. ✉email: snowlee@zju.edu.cn; TangYB0303@163.com

in adipose tissue<sup>16</sup>. Elevated levels of adipose tissue RAS have been documented in various models of obesity induced by high-fat diets (HFD)<sup>17</sup>. Studies have demonstrated dysregulation of the RAS in cases of intestinal inflammation, with drugs designed to modulate the RAS showing efficacy in various animal models of colitis<sup>18–20</sup>. RAS inhibitors, including angiotensin-converting enzyme inhibitors (ACE-I) and angiotensin receptor blockers (ARB), are considered safe antihypertensive treatments with additional anti-inflammatory and anti-fibrotic effects<sup>21</sup>. These inhibitors can positively impact IBD by addressing inflammation, leukocyte recruitment, and fibrosis. In the context of obesity, adipocytes secrete substantial amounts of angiotensinogen (AGT), leading to the activation of both systemic and local RAS, which in turn modulate obesity and inflammation<sup>22</sup>. However, the complex interplay between obesity, IBD, and RAS remains incompletely understood. In this study, we provide robust evidence that obesity activates the local RAS, leading to increased permeability of the intestinal epithelial barrier and exacerbation of experimental colitis in murine models. We anticipate that these findings will significantly enhance the molecular understanding of obesity's role in colitis pathogenesis and contribute to the advancement of clinical management strategies for colitis.

Methods  
Animals and treatment

Male C57BL/6J mice, aged 6–8 weeks (18–20 g), were housed under strict light/dark cycles (12 h each) at room temperature with food and water provided ad libitum. These mice were purchased from GemPharmatech Co., Ltd. (Jiangsu, China), with the license number: SCKK (Su) 2023-0009. The mice were fed either a high-fat diet (HFD; TP-23520, Trophic Diet, China), containing 60% of available energy as fat, or a low-fat diet (LFD; TP-23524, Trophic Diet, China), containing 10% of available energy as fat, for 10 weeks. The physical composition of the diets is shown in Table 1. Following dietary treatment, experimental colitis was induced using 2,4,6-trinitrobenzenesulfonic acid (TNBS; Sigma-Aldrich) according to a previously described protocol<sup>23</sup>. In some experiments, to assess the effect of AT1 receptor blockade on colitis development, mice were treated with losartan dissolved in drinking water at 10 mg/ml for 14 days. On day 7 after starting losartan treatment, the mice were anesthetized with 100 mg/kg ketamine and then treated with TNBS. Specifically, mice were presensitized with a 1% TNBS solution. After mixing acetone and olive oil in a 4:1 ratio, the mixture was combined with 5% TNBS in a 4:1 ratio to prepare the 1% TNBS sensitizing solution. The mice's backs were shaved, creating an area of approximately 1.5 × 1.5 cm. Then, 150 µl of the sensitizing solution was evenly applied to the shaved area on the mice's backs to ensure full absorption. After 8 days, following an overnight fast, the experimental groups were administered 0.1 mL of a solution containing 5% TNBS and absolute ethanol (1:1) via intrarectal injection, while the control groups received a treatment of 50% ethanol<sup>24</sup>. Body weight, stool consistency, and rectal bleeding were monitored for 3 days. Subsequently, the mice were euthanized by inhalation of excess CO<sub>2</sub>, and colons were harvested for histological and biochemical analyses. Clinical scores were assessed in detail as described previously<sup>25</sup>. The colonic mucosa were scraped, and total RNA and proteins were isolated. A total of 20 mice were sacrificed in this experiment. All methods were performed in accordance with the relevant guidelines and regulations. All animal studies were approved by the Institutional Ethical Committee of Zhejiang Provincial People's Hospital (20240722210638164444). This study is reported in compliance with the ARRIVE guidelines.

Assessment of lipids

After 10 weeks of dietary treatment, blood and colon samples were collected from the mice for lipid measurement. To a glass centrifuge tube containing fresh or frozen microalgal paste or pulverized dry algal biomass, 8 ml of a 2:1 chloroform–methanol (v/v) mixture was added. The biomass was manually resuspended by vigorously shaking the tube for a few seconds, followed by the addition of 2 ml of a 0.73% NaCl aqueous solution. Phase separation was achieved by centrifuging for 2 min at 350 g, and the lower phase was collected for analysis<sup>26</sup>. The extracted lipids were allowed to air-dry and were then weighed. Triglyceride (F005-2-1), cholesterol (A111-2-1), and non-esterified free fatty acid (A042-2-1) contents were quantified using commercial assay kits from Nanjing Jiancheng Bioengineering Institute, China, in accordance with the manufacturer's instructions.

Ingredient	High-fat diet (g/kg)	Low-fat diet (g/kg)
Casein	258	190
Cystine	4	3
Corn starch	0	299
Dextrin	162	3
Sucrose	89	332
Cellulose	65	47
Soybean oil	32	24
Lard	317	19
Mineral and vitamin mixture	71	52
Choline tartrate	3	2
TBHQ	0.07	0.01
Total	1000	1000

Table 1. Physical composition of the diets.

### ELISA assay

Whole blood was collected from mice via cardiac puncture and allowed to rest at room temperature for 30 min. The blood was then centrifuged at 3000 rpm for 20 min to obtain the supernatant. Serum TNF- $\alpha$  levels were measured using a mouse TNF- $\alpha$  ELISA kit (Solarbio, Beijing, China) according to the manufacturer's guidelines.

### Measurement of colonic permeability

Colonic permeability was assessed by measuring serum FITC-dextran levels. Mice were fasted for 6 h and then orally administered 200 mg/kg of 4000 Da FITC-dextran. Serum samples were collected 2 h later and analyzed using an M200 TECAN microplate reader at a wavelength of 530 nm to evaluate colonic mucosal permeability *in vivo*.

### Histological analysis

After euthanasia, the colon was immediately collected from the mice and fixed in 4% formaldehyde prepared in PBS (pH 7.2–7.4) overnight at 4 °C. The samples were then processed and embedded in paraffin wax in a “Swiss roll” configuration and sectioned into 5  $\mu$ m slices. Colonic tissue morphology was assessed by staining sections with hematoxylin and eosin (H&E), and histological scores were recorded according to a previously described scoring system<sup>27</sup>.

### Flow cytometry

Mouse colonic lamina propria cells were isolated, and fluorescence-activated cell sorting (FACS) analysis was conducted. The following antibodies were used in the flow cytometry assays: anti-mouse CD3e APC (152305), anti-mouse CD4 FITC (100406), and anti-mouse IL-17A APC/cy7 (506940), all purchased from Biolegend. FACS analysis was performed using the FACSCanto II system (BD Biosciences).

### Western blot analysis

The Western blot assay was performed following Good Clinical Laboratory Practice standards. Proteins were first separated using SDS-PAGE and then transferred to polyvinylidene fluoride (PVDF) membranes. The membranes were incubated with primary antibodies targeting occludin (ab-216327, Abcam), AT1R (ab124734, Abcam), angiotensinogen (AGT) (sc-374511, Santa Cruz Biotechnology), renin (sc-133145, Santa Cruz Biotechnology), and GAPDH (5174, Cell Signaling Technology) at a 1:1000 dilution. Subsequently, the appropriate secondary antibodies—Goat Anti-Rat (98164S, Cell Signaling Technology) and Goat Anti-Mouse (91196S, Cell Signaling Technology)—were applied at a 1:2000 dilution. Chemiluminescent detection was then performed using the Beyotime P0018S kit. For the Western blot quantification, we used Image J software for grayscale analysis.

### qRT-PCR

The qRT-PCR reaction was conducted according to the manufacturer's instructions. Total RNA was extracted from colonic mucosa using TRIzol reagent (Invitrogen). First-strand cDNA synthesis was carried out with the PrimeScript RT Reagent Kit (TaKaRa, Mountain View, CA). Real-time PCR was performed using the SYBR Premix Ex Taq Kit (TaKaRa) on an ABI 7500 real-time system. Fold change was calculated using the  $2^{-\Delta\Delta CT}$  method, with GAPDH as an internal control. PCR primers are listed in Table 2.

### Statistical analysis

Data are presented as mean with SD or median with IQR. Statistical analyses were performed using an unpaired two-tailed Student's *t*-test for comparisons between two groups and one-way analysis of variance (ANOVA) with a Student–Newman–Keuls post hoc test for comparisons between three or more groups. Qualitative data are reported as frequencies and percentages. Statistical analyses were conducted using SAS version 9, with a significance level set at  $p < 0.05$ .

## Results

### Long-term HFD feeding induces obesity in C57BL/6 mice

C57BL/6 mice were fed an HFD for 10 weeks to establish an obesity model. As shown in Fig. 1, at the end of this dietary treatment, the HFD-fed mice exhibited greater weight gain (Fig. 1A) and elevated levels of triglycerides (Fig. 1B), total cholesterol (Fig. 1C), free fatty acids (FFA) (Fig. 1D), and TNF- $\alpha$  (Fig. 1E) in their plasma compared to mice fed a LFD. These results confirm the successful establishment of the obesity model in C57BL/6 mice through long-term high-fat diet feeding. Additionally, triglyceride levels in the colonic contents were notably increased in the obesity model group (Fig. 1F), which may contribute to elevated levels of pro-inflammatory cytokines and chemokines, such as TNF- $\alpha$  in the intestine. This cascade of events could exacerbate colitis progression, suggesting a potential association between obesity and increased susceptibility to colitis.

### HFD-induced obesity exacerbates the progression of experimental colitis

TNBS treatment resulted in a reduction in body weight in mice over a 3 day period, with more pronounced weight loss observed in the model mice compared to the control groups (Fig. 2A). Compared to the LFD group, the intestines of HFD-fed mice appeared thinner and exhibited a pallid coloration throughout. Colitis manifestations following TNBS treatment included colon shortening, swelling, bleeding, and ulcer formation, with HFD-fed mice displaying more severe symptoms than the LFD-fed group (Fig. 2B). Semiquantitative assessment of these colons showed higher clinical scores in HFD-fed mice compared to LFD-fed mice (Fig. 2C). Histological analysis demonstrated that mice fed a high-fat diet (HFD) displayed colonic mucosal atrophy compared to those on a low-fat diet (LFD). Furthermore, HFD-fed mice exhibited more severe ulceration, characterized by larger and more numerous ulcers in H&E-stained sections, along with significantly lower histological scores following

Name	Species	Forward and reverse primer sequence (5'→3')
GAPDH	Mus musculus	TGTGTCCGTCGTGGATCTGA
		CCTGCTTCACCACCTTCTTGA
Tnfa	Mus musculus	TCAGCCTCTTCTCATTCCTG
		CAGGCTTGTCACCTCGAATTT
Ifng	Mus musculus	GCGTCATTGAATCACACCTG
		TGAGCTCATTGAATGCTTGG
Il6	Mus musculus	ATAGTCCTTCCTACCCCAATTTCC
		CTGACCACAGTGAGGAATGTCCAC
Agtr1	Mus musculus	CTGCTCTCCCGACTTAACA
		CTGCTCTCCCGACTTAACA
Ren	Mus musculus	GAGGCCTTCCTTGACCAATC
		TGTGAATCCCAAGCAAGG
Agt	Mus musculus	TCTTTGGCACCTGGTCTCTTCT
		TTCTCAGTGGCAAGAACTGGGTCA
Agtr2	Mus musculus	GCCAACATTTTATTCCGGGA
		CCACTGAGCATATTCTCGGG
Mas1	Mus musculus	CATCTAGGACTGGGCAGAGC
		AGTCAGGAGGTGGAGAGCA

**Table 2.** Primers for RT-qPCR.

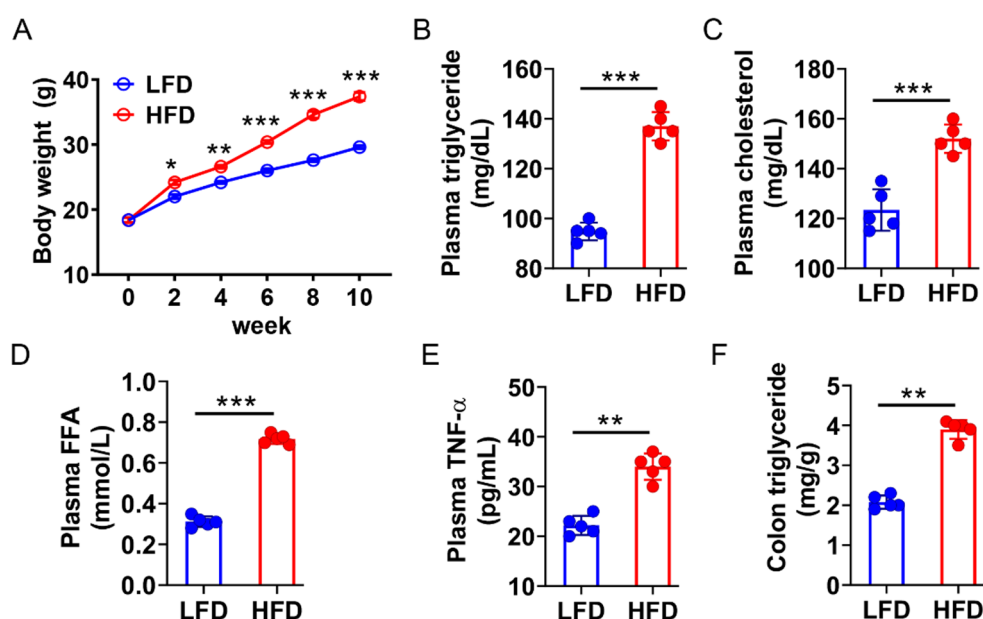


**Fig. 1.** Long-term HFD feeding induces obesity in C57BL/6 mice. **(A)** Changes in body weight of mice fed a low-fat diet (LFD) or high-fat diet (HFD) for 10 Weeks. \* $P < 0.05$ , \*\* $P < 0.01$ , \*\*\* $P < 0.001$  versus LFD;  $n = 5$  each group. **(B)** Triglyceride content in the plasma of LFD-fed or HFD-fed mice. \*\*\* $P < 0.001$  versus LFD;  $n = 5$  each group. **(C)** Cholesterol content in the plasma of LFD-fed or HFD-fed mice. \*\*\* $P < 0.001$  versus LFD;  $n = 5$  each group. **(D)** Free fatty acid (FFA) content in the plasma of LFD-fed or HFD-fed mice. \*\*\* $P < 0.001$  versus LFD;  $n = 5$  each group. **(E)** TNF- $\alpha$  content in the plasma of LFD-fed or HFD-fed mice. \*\* $P < 0.01$  versus LFD;  $n = 5$  each group. **(F)** Triglyceride content in colonic mucosa of LFD-fed or HFD-fed mice. \*\* $P < 0.01$  versus LFD;  $n = 5$  each group.

TNBS induction (Fig. 2D,E). Additionally, the study revealed elevated levels of pro-inflammatory cytokines and chemokines (TNF- $\alpha$ , IL-6) in the colonic mucosa of HFD-fed mice compared to LFD-fed controls. Furthermore, long-term HFD combined with TNBS treatment induced a significant upregulation of TNF- $\alpha$ , IL-6, and IFN- $\gamma$  in the colonic mucosa relative to the LFD group. (Fig. 2F). These findings suggest that prolonged HFD consumption may lead to lipid accumulation in the intestine, resulting in heightened inflammatory responses and exacerbation of colitis progression in TNBS-induced experimental colitis.

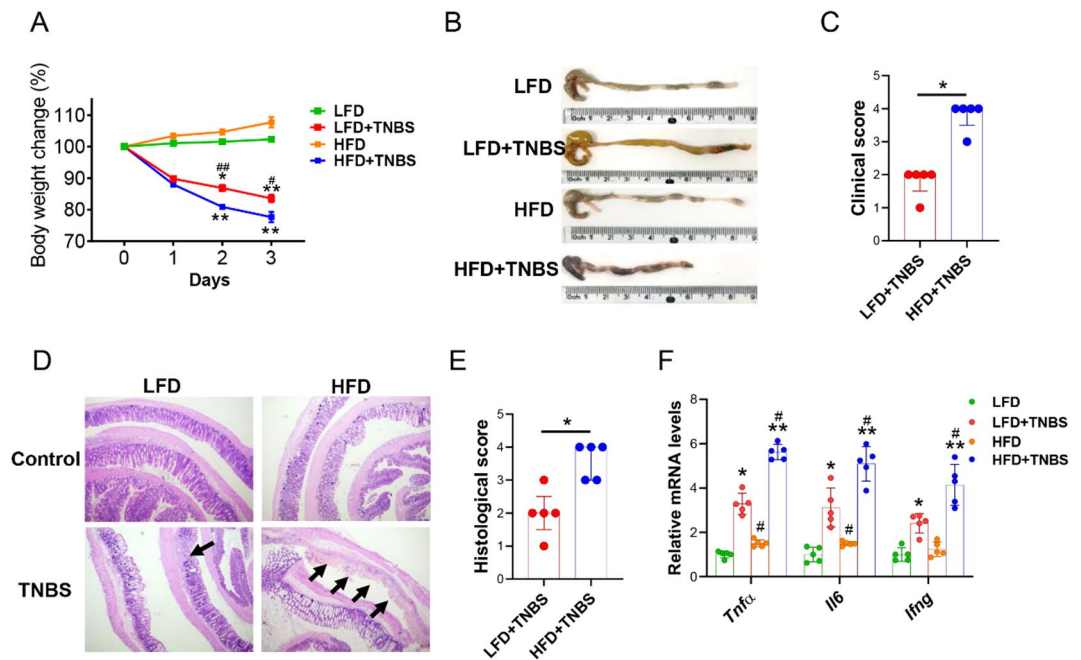


**Fig. 2.** HFD-induced obesity exacerbates the progression of experimental colitis. **(A)** Body weight changes in mice fed a low-fat diet (LFD) or HFD for 10 wk following 2,4,6-trinitrobenzenesulfonic acid (TNBS) treatment. \* $P < 0.05$ , \*\* $P < 0.01$  versus respective LFD or HFD; # $P < 0.05$ , ## $P < 0.01$  versus LFD + TNBS;  $n = 5$  each group. **(B)** Gross morphology of the colons on day 3 after TNBS treatment. **(C)** Clinical score of the colons on day 3 after TNBS treatment. \* $P < 0.05$  versus LFD + TNBS;  $n = 5$  each group. **(D)** Hematoxylin and eosin histology of the colons on day 3 after TNBS treatment (arrows point to the ulcerated area; magnification:  $\times 50$ ). **(E)** Histological score of the colons on day 3 after TNBS treatment. \* $P < 0.05$  versus LFD + TNBS;  $n = 5$  each group. **(F)** Real-time PCR quantitation of pro-inflammatory cytokines and chemokines in colonic mucosa on day 3 after TNBS treatment. \* $P < 0.05$ , \*\* $P < 0.01$  versus LFD or HFD; # $P < 0.05$  versus LFD or LFD + TNBS;  $n = 5$  each group.

### HFD-induced obesity exacerbates local RAS activation in the colon of mice treated with TNBS

The RAS has been found to play a significant role in the pathogenesis of colitis. Garg et al.<sup>28</sup> demonstrated that key components of the RAS are expressed in the intestinal tract and may contribute to inflammation and fibrosis in IBD. Their research suggests that ACE inhibitors and angiotensin II receptor blockers (ARBs) could offer potential therapeutic benefits for patients with IBD, and further investigation is needed to assess the efficacy of this novel treatment approach. Accordingly, we hypothesized that obesity may exacerbate colitis development by activating the RAS pathway. To investigate this, we assessed the local expression of RAS components in the colon of experimental models. Western blot analysis of colonic mucosal lysates revealed a significant increase in AT1R, AGT, and renin levels in the colon of HFD-fed mice compared to LFD-fed mice, particularly following TNBS treatment (Fig. 3A,B). Additionally, qRT-PCR analysis showed a significant upregulation of mRNA levels for these genes in HFD-fed mice compared to LFD-fed mice (Fig. 3C). We found that levels of Mas1 (MasR) were significantly elevated in HFD-fed mice, especially in those treated with TNBS, compared to mice on a LFD diet. We hypothesize that obesity-related conditions—such as a high-fat diet and metabolic dysregulation—may disrupt the ACE2/Ang1-7/MasR axis, leading to MasR upregulation. Alternatively, chronic AT1R overactivation in obesity may trigger a compensatory rise in MasR expression to counteract the deleterious effects of Ang II. In contrast, the Agtr2 (AT2R) gene, known for its anti-inflammatory properties, was downregulated in HFD-fed mice, particularly in those treated with TNBS. (Fig. 3D). These findings suggest that prolonged HFD consumption enhances activation of the local RAS in the colon, which may contribute to the exacerbation of colitis progression.

### Long-term HFD increases intestinal permeability in TNBS-treated mice.

Mehandru et al.<sup>29</sup> observed that in IBD, there is impairment of intestinal epithelial barrier function, with alterations in tight junctions and increased intestinal permeability serving as significant markers. In our study, intestinal permeability was assessed using FITC-dextran gavage test. FITC-dextran feeding assays revealed that mice fed a HFD and treated with TNBS had a significantly higher plasma concentration of FITC-dextran compared to mice fed a LFD and treated with TNBS, indicating worsened intestinal permeability in the HFD-fed mice following TNBS induction (Fig. 3E). Additionally, Western blot analysis of colonic mucosal lysates revealed a reduction in occludin expression following TNBS treatment. Consistent with the findings on intestinal permeability, the decrease in occludin was significantly greater in mice subjected to a prolonged HFD compared



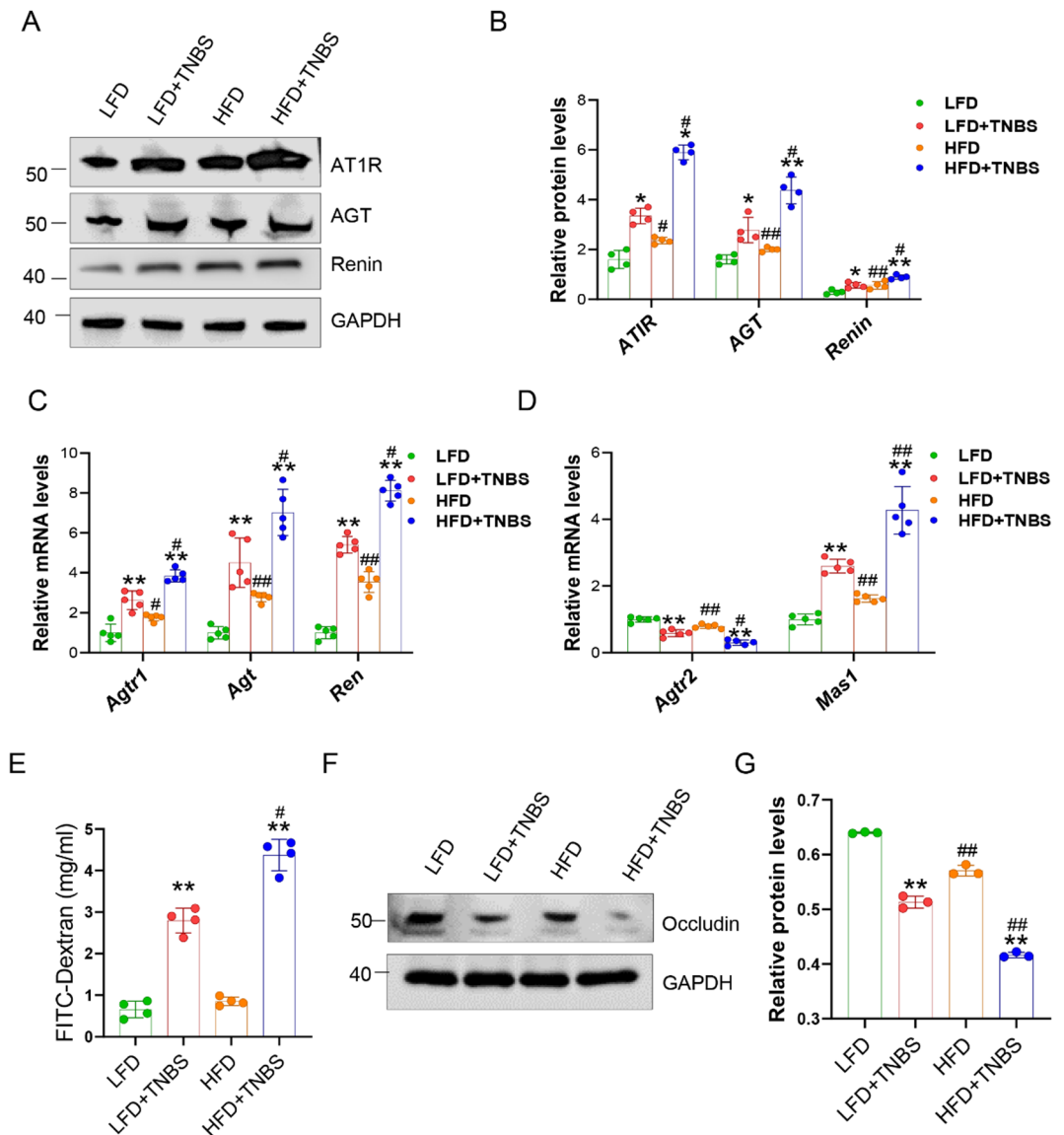


**Fig. 3.** HFD-induced obesity exacerbates local RAS activation and intestinal permeability in the colon of mice treated with TNBS. **(A)** Representative Western blot of major components of the RAS in colonic mucosa on day 3 after TNBS treatment. **(B)** Densitometric quantitation of major components of the RAS in colonic mucosa on day 3 after TNBS treatment. \* $P < 0.05$ , \*\* $P < 0.01$  versus LFD or HFD; # $P < 0.05$ , ## $P < 0.01$  versus LFD or LFD TNBS;  $n = 4$  each group. **(C)** Real-time PCR quantitation of *Agtr1*, *Agt* and *Ren* in colonic mucosa on day 3 after TNBS treatment. \*\* $P < 0.01$  versus LFD or HFD; # $P < 0.05$ , ## $P < 0.01$  versus LFD or LFD TNBS;  $n = 5$  each group. **(D)** Real-time PCR quantitation of *Agtr2* and *Mas1* in colonic mucosa on day 3 after TNBS treatment. \*\* $P < 0.01$  versus LFD or HFD; ## $P < 0.01$  versus LFD or LFD TNBS;  $n = 5$  each group. **(E)** Quantitation of paracellular FITC-dextran passage across mucosal barrier in mice. \*\* $P < 0.01$  versus low-fat diet (LFD) or HFD; # $P < .05$  versus LFD TNBS;  $n = 4$  each group. **(F)** Western blot analyses of occludin in colonic mucosal lysates. **(G)** Densitometric quantitation of occludin in colonic mucosal lysates. \*\* $P < 0.01$  versus LFD or HFD; ## $P < 0.01$  versus LFD or LFD TNBS;  $n = 3$  each group. Only representative blots are shown.

to those on a LFD (Fig. 3F,G). This difference may be a key factor contributing to the compromised integrity of intestinal epithelial tight junctions and damage to the mucosal epithelial barrier.

#### Blockade of AT1 receptor signaling ameliorates experimental colitis induced by long-term HFD.

To confirm RAS activation by long-term HFD, diet-induced obese mice were treated in the presence or absence of losartan (LST) (10 mg/ml) for 14 days (Fig. 4A) and, which blocked AT1 receptor signaling. As can be seen in Fig. 5, losartan effectively reduced body weight loss (Fig. 4B) and decreased histological injuries, such as colonic swelling, shortening, bleeding, and ulceration, in obese mice with TNBS-induced colitis (Fig. 4C,E). Additionally,

both clinical and histological scores decreased significantly in the group treated with losartan (Fig. 4D,F). Mice treated with losartan also exhibited reduced levels of pro-inflammatory cytokines and chemokines (TNF- $\alpha$ , IL-6, IFN- $\gamma$ ) in the colonic mucosa (Fig. 4G). Losartan also significantly reduced the expression of AT1R and renin while increasing AT2R expression in the colonic mucosa of mice (Fig. 4H).

These findings suggest that blocking AT1 receptor signaling with losartan effectively mitigates TNBS-induced colitis in mice subjected to a long-term HFD, indicating a potential link between the RAS and obesity.

### Blockade of AT1 receptor signaling ameliorates intestinal permeability and Th17 cells expression under long-term HFD.

To explore the mechanism by which losartan alleviates TNBS-induced colitis in obese mice on a long-term HFD, intestinal permeability was assessed across different groups. The experimental group treated with losartan showed a significant decrease in intestinal permeability compared to the control group that did not receive losartan (Fig. 5A), which aligns with the clinical and pathological changes observed in Fig. 4. Additionally, losartan treatment mitigated the TNBS-induced reduction in occludin in the intestinal epithelium, as shown by western blot analysis of colonic mucosal lysates (Fig. 5B,C). We found an increase in CD4<sup>+</sup> Th17 cells in the lamina propria of mice fed a HFD, especially in mice treated with TNBS. However, the expression of CD4<sup>+</sup>Th17

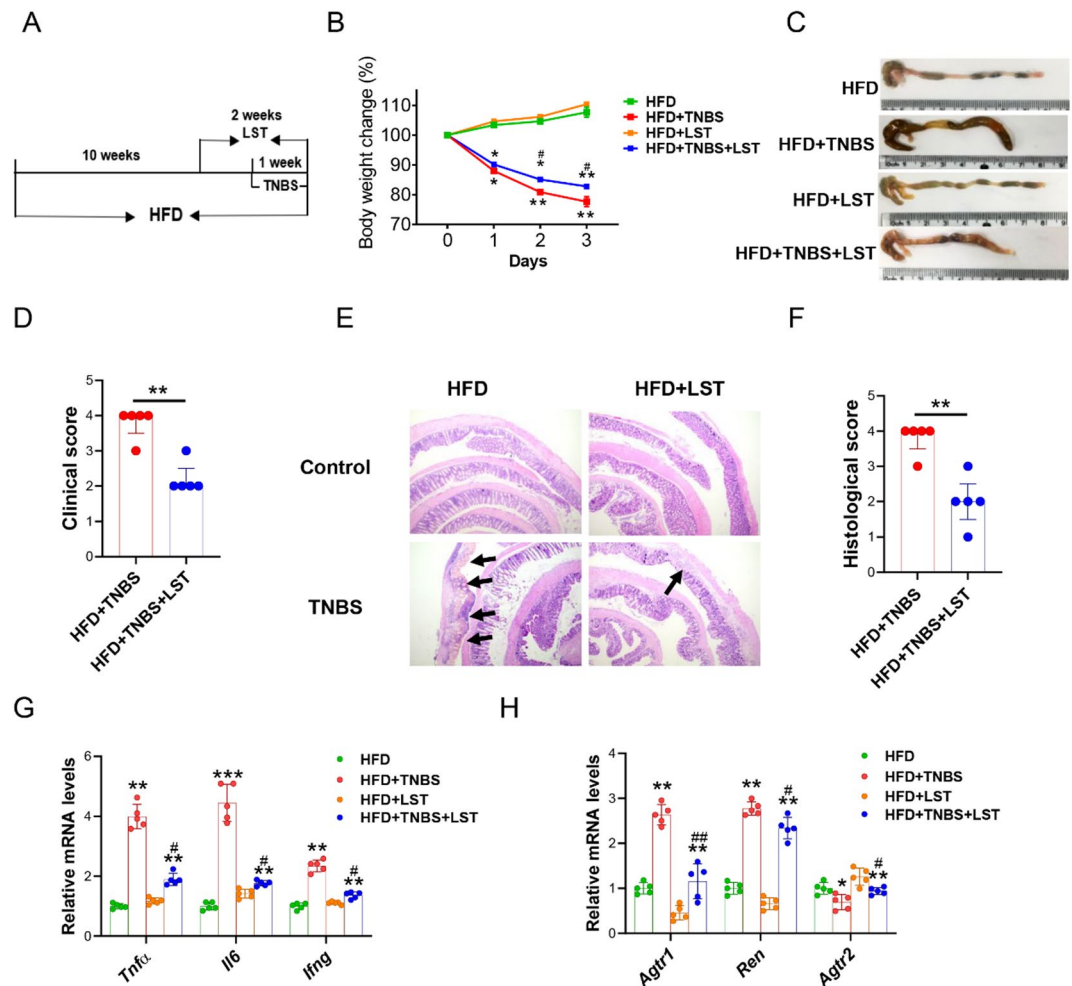


**Fig. 4.** Blockade of AT1 receptor signaling ameliorates experimental colitis induced by long-term HFD. (A) Workflow diagram. (B) Body weight changes in mice on HFD-TNBS following losartan treatment. \* $P < 0.05$ , \*\* $P < 0.01$  versus respective HFD or HFD LST; # $P < 0.05$ , versus HFD TNBS;  $n = 5$  each group. (C) Gross morphology of the colons in mice following losartan treatment. (D) Clinical score of the colons in mice following losartan treatment. \*\* $P < 0.01$  versus HFD TNBS;  $n = 5$  each group. (E). Hematoxylin and eosin histology of the colons in mice following losartan treatment (arrows point to the ulcerated area; magnification:  $\times 50$ ). (F). Histological score of the colons in mice following losartan treatment. \*\* $P < 0.01$  versus HFD TNBS;  $n = 5$  each group. (G) Real-time PCR quantitation of pro-inflammatory cytokines and chemokines in colonic mucosa following losartan treatment. \*\* $P < 0.01$ , \*\*\* $P < 0.001$  versus respective HFD or HFD LST; # $P < 0.05$ , versus HFD TNBS;  $n = 5$  each group. (H) Real-time PCR quantitation of Agtr1, Ren and Agtr2 in colonic mucosa on day 3 after TNBS treatment. \* $P < 0.05$ , \*\* $P < 0.01$  versus respective HFD or HFD LST; # $P < 0.05$ , # $P < 0.01$  versus HFD TNBS;  $n = 5$  each group.

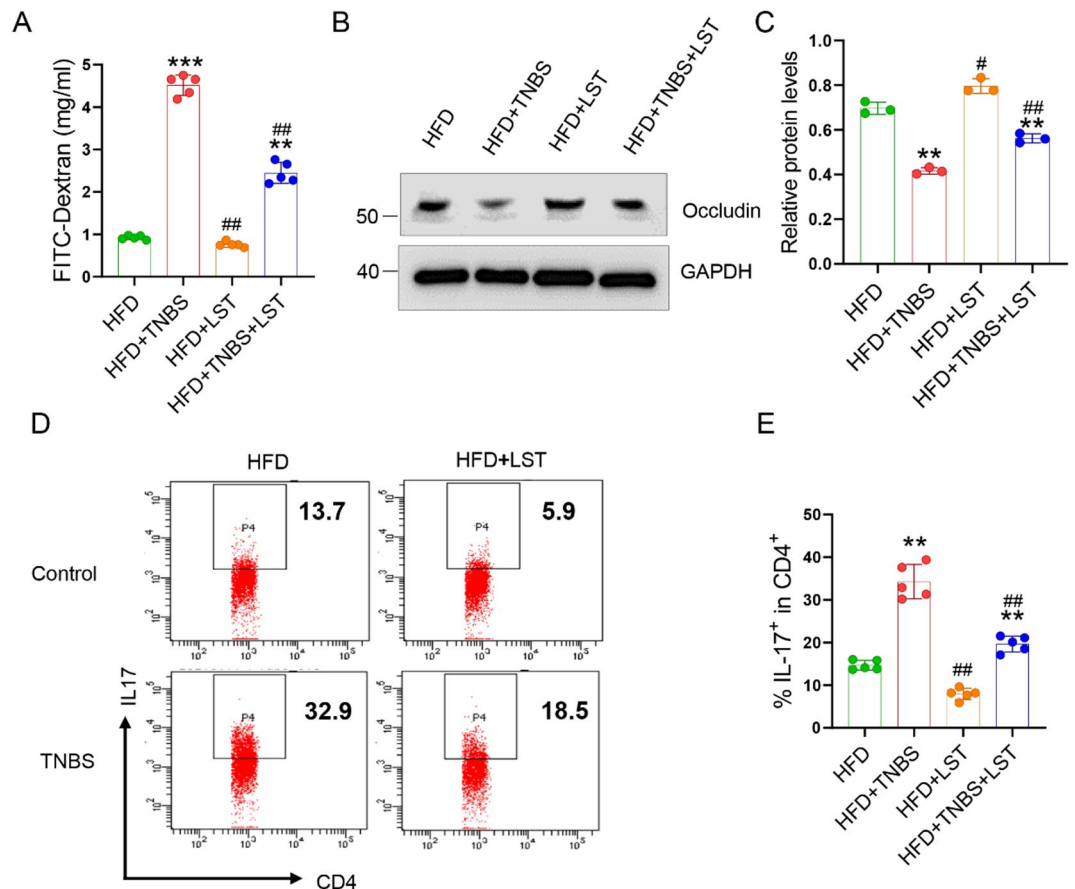


**Fig. 5.** Blockade of AT1 receptor signaling ameliorates intestinal permeability and Th17 cells expression under long-term HFD. **(A)** Quantitation of paracellular FITC-dextran passage across mucosal barrier in mice.  $^{**}P < 0.01$ ,  $^{***}P < 0.001$  versus respective HFD or HFD LST;  $^{##}P < 0.01$ , versus HFD TNBS;  $n = 5$  each group. **(B)** Western blot analyses of occludin in colonic mucosal lysates. **(C)** Densitometric quantitation of occludin in colonic mucosal lysates.  $^{**}P < 0.01$  versus respective HFD or HFD LST;  $^{##}P < 0.01$  versus HFD or HFD TNBS;  $n = 3$  each group. Only representative blots are shown. **(D)** Representative FACS plots for Th17 cells in the colonic lamina propria. **(E)** Quantitation of Th17 cells.  $^{**}P < 0.01$  versus respective HFD or HFD LST;  $^{##}P < 0.01$  versus HFD or HFD TNBS.  $n = 5$  per group.

cells was significantly reduced after treatment with losartan (Fig. 5D,E). These results suggest that inhibiting AT1 receptor signaling with losartan effectively ameliorates TNBS-induced colitis by reducing intestinal permeability, enhancing the colonic mucosal epithelial barrier, and decreasing the expression of CD4<sup>+</sup> Th17 cells.

## Discussion

Dietary fat plays a crucial role in the development of intestinal diseases<sup>30</sup>. This interest is particularly focused on the molecular mechanisms through which obesity-induced intestinal permeability contributes to the progression of IBD<sup>14</sup>. Adipose tissue plays a crucial role in energy homeostasis; however, excessive macronutrient intake and metabolic dysfunction can lead to pathological expansion of visceral adipose tissue<sup>31</sup>. This expansion promotes the production of monocyte chemoattractants, leading to the infiltration of adipose tissue by circulating monocytes, which then differentiate into macrophages. These macrophages secrete various pro-inflammatory cytokines, including TNF- $\alpha$ , IL-1 $\beta$ , and IL-6, thereby driving chronic, low-grade systemic inflammation<sup>32</sup>. In this study, we observed that HFD-induced obese mice exhibited more expression levels of TNF- $\alpha$ , IL-6, and IFN- $\gamma$  within the colonic mucosa. These factors are critical regulators of tight junction integrity and are significant risk factors for increased intestinal permeability<sup>33</sup>.

The integrity of the intestinal barrier is known to be highly sensitive to the inflammatory state of the intestine. Under homeostatic conditions, the intestine employs various mechanisms to prevent the translocation of foreign substances from the lumen to the lamina propria. Tight junctions (TJs) between intestinal epithelial cells are composed of a complex array of proteins, including occludin, claudin. These proteins collectively regulate intestinal permeability by modulating ion flux, small molecule transport, and solute selectivity, thereby maintaining the separation between the lamina propria and the lumen<sup>30</sup>. This regulatory function is crucial in the pathogenesis of IBD<sup>34</sup>. Occludin, a key protein within intestinal epithelial tight junctions, is essential for maintaining the integrity of the intestinal barrier. Its primary role is in stabilizing tight junctions rather than their initial assembly<sup>33</sup>. Severe impairment of occludin expression has been documented in disease models of



intestinal inflammation<sup>35</sup>. Our data indicate that HFD-induced obesity significantly increases colonic mucosal permeability in TNBS colitis model mice, which is associated with a marked reduction in occludin protein expression. This suggests a compromise in the integrity of epithelial tight junctions. The precise molecular mechanisms underlying the increased mucosal permeability observed in obese individuals are yet to be fully elucidated. Dietary components may also influence intestinal permeability and the severity of colitis in murine models through their interactions with the gut microbiota<sup>36</sup>. The disruption of the intestinal mucosal barrier is crucial for the unwanted interaction between antigens and the immune system, leading to inflammation<sup>14</sup>. It is well-established that a fully functional RAS exists in both animal and human adipose tissue, playing a crucial role in the regulation of body fat and thus representing a significant factor in the pathophysiology of obesity<sup>37</sup>. Conversely, obesity itself can lead to overactivation of the RAS<sup>22</sup>. For instance, Rahmouni et al.<sup>38</sup> demonstrated that obesity induced by a HFD resulted in increased expression of AGT genes in intra-abdominal adipose tissue in both mice and humans. Rasha et al.<sup>39</sup> proposed through a literature review that obesity activates the RAS and induces angiotensin II secretion, which may contribute to both local and systemic inflammation in breast adipose tissue and is associated with breast cancer. RAS antagonists are increasingly seen as key to addressing the growing issues of obesity and insulin resistance<sup>40</sup>. Emerging data also suggest a potential role for the RAS in IBD. For instance, it was found that a genetic mouse model with angiotensinogen knockout displayed milder disease in TNBS-induced colitis, along with reduced production of pro-inflammatory cytokines and increased production of anti-inflammatory cytokines in the colon. This indicates that the RAS is involved in the immune regulation of the colon. Shi et al.<sup>24</sup> used a renin transgenic mouse model to show that overexpression of renin significantly increases susceptibility to colitis, a process highly dependent on active renin and independent of high blood pressure. However, the exact mechanism linking the RAS to colitis remains unclear. The local RAS in the gastrointestinal tract exerts pleiotropic effects through various signaling pathways, which may play a crucial role in the pathogenesis of IBD. Additionally, angiotensin II (Ang II) promotes T-helper 1 (Th1) and T-helper 17 (Th17) mediated autoimmunity, further contributing to IBD pathogenesis. Ang II can directly stimulate the Th1/Th17 immune response in epithelial cells via colonic dendritic cells, thereby inducing Th17 and Th1/Th17 cell differentiation and mediating autoimmune responses<sup>24</sup>. Furthermore, Lee et al.<sup>41</sup> identified the RAS as a potential mediator of colonic inflammation, which can exacerbate IBD by activating the NF- $\kappa$ B signaling pathway. This pathway regulates various pro-inflammatory genes essential for the inflammatory response. Notably, the ACE inhibitor enalapril has been shown to mitigate this pro-inflammatory effect.

In this study, we investigated the impact of obesity on the development of colitis using a TNBS-induced model, which closely mimics CD. Obesity was induced in mice by feeding them a HFD. Our findings show that obesity resulting from prolonged HFD feeding exacerbates tight junction damage in the colonic epithelium of colitis-afflicted mice. This condition significantly increases mucosal permeability, compromises the integrity of the intestinal epithelial barrier, and worsens experimental colitis. These effects are, at least in part, attributed to excessive activation of the local RAS. Further experiments demonstrated that losartan, an AT1 receptor antagonist, effectively reverses the damage caused by obesity, validating our hypothesis that obesity exacerbates experimental colitis in mice through local RAS activation. Our research highlights that obesity significantly increases the risk of developing colitis, with the gut RAS playing a critical role in this relationship. Therefore, future research should focus on exploring diverse therapeutic interventions, including nutritional therapy, obesity management strategies, and pharmacological agents targeting the RAS.

## Data availability

No datasets were generated or analysed during the current study. The datasets used and/or analysed during the current study are available from the corresponding author on reasonable request.

Received: 25 March 2025; Accepted: 8 September 2025

Published online: 10 October 2025

## References

- Ng, S. C. et al. Worldwide incidence and prevalence of inflammatory bowel disease in the 21st century: A systematic review of population-based studies. *The Lancet* **390**(10114), 2769–2778 (2017).
- Wu, Z. et al. Gut microbiota from green tea polyphenol-dosed mice improves intestinal epithelial homeostasis and ameliorates experimental colitis. *Microbiome* **9**(1), 184 (2021).
- Kaminsky, L. W., Sadi, R. A. & Ma, T. Y. IL-1 $\beta$  and the intestinal epithelial tight junction barrier. *Front. Immunol.* **12**, 767456 (2021).
- Cremonini, E. et al. (-)-Epicatechin protects the intestinal barrier from high fat diet-induced permeabilization: Implications for steatosis and insulin resistance. *Redox Biol.* **14**, 588–599 (2018).
- Lin, L. et al. Multi-omics analysis of western-style diet increased susceptibility to experimental colitis in mice. *J. Inflamm. Res.* <https://doi.org/10.2147/JIR.S361039> (2022).
- Ananthakrishnan, A. N. Epidemiology and risk factors for IBD. *Nat. Rev. Gastroenterol. Hepatol.* **12**(4), 205–217 (2015).
- Rizzello, F., Spisni, E., Giovannardi, E., Imbesi, V. & Gionchetti, P. J. N. Implications of the Westernized Diet in the Onset and Progression of IBD. *Nutrients* **11**, 1033 (2019).
- Chapman-Kiddell, C. A., Davies, P. S., Gillen, L. & Radford-Smith, G. L. Role of diet in the development of inflammatory bowel disease. *Inflamm. Bowel Dis.* **16**(1), 137–151 (2010).
- Paik, J., Fierce, Y., Treuting, P. M., Brabb, T. & Maggio-Price, L. J. High-fat diet-induced obesity exacerbates inflammatory bowel disease in genetically susceptible Mdr1a<sup>-/-</sup> male mice. *J. Nutr.* **143**, 1240–1247 (2013).
- Chobot, A., Górowska-Kowolik, K., Sokołowska, M. & Jarosz-Chobot, P. Obesity and diabetes: Not only a simple link between two epidemics. *Diabet./Metab. Res. Rev.* **34**(7), e3042 (2018).
- Winer, D. A., Luck, H., Tsai, S. & Winer, S. The intestinal immune system in obesity and insulin resistance. *Cell Metab.* **23**(3), 413–426 (2016).
- Cani, P. D. et al. Changes in gut microbiota control metabolic endotoxemia-induced inflammation in high-fat diet-induced obesity and diabetes in mice. *Diabetes* **57**(6), 1470–1481 (2008).

13. Shen, W. et al. Intestinal and systemic inflammatory responses are positively associated with Sulfidogenic bacteria abundance in high-fat-fed male C57BL/6J mice. *J. Nutr.* **144**(8), 1181–1187 (2014).
14. Ahmad, R., Rah, B., Bastola, D., Dhawan, P. & Singh, A. B. Obesity-induces organ and tissue specific tight junction restructuring and barrier deregulation by Claudin switching. *Sci. Rep.* **7**(1), 1–16 (2017).
15. Cox, A. J., West, N. P. & Cripps, A. W. Obesity, inflammation, and the gut microbiota. *Lancet Diab. Endocrinol.* **3**(3), 207–215 (2015).
16. Yvan-Charvet, L. & Quignard-Boulangé, A. Role of adipose tissue renin–angiotensin system in metabolic and inflammatory diseases associated with obesity. *Kidney Int.* **79**(2), 162–168 (2011).
17. Sarzani, R. et al. Renin–angiotensin system, natriuretic peptides, obesity, metabolic syndrome, and hypertension: An integrated view in humans. *J. Hypertens.* **26**(5), 831–843 (2008).
18. Lei, et al. The renin–angiotensin system promotes colonic inflammation by inducing T<sub>H</sub>17 activation via the JAK2/STAT pathway. (2019).
19. Zhang, Q. et al. Overexpression of a wheat  $\alpha$ -amylase type 2 impact on starch metabolism and abscisic acid sensitivity during grain germination. *Plant J.* **108**(2), 378–393 (2021).
20. Inokuchi, Y. J. Amelioration of 2,4,6-trinitrobenzene sulphonic acid induced colitis in angiotensinogen gene knockout mice. *Gut* **54**, 349–356 (2005).
21. Salmenkari, H., Korpela, R. & Vapaatalo, H. Renin–angiotensin system in intestinal inflammation: Angiotensin inhibitors to treat inflammatory bowel diseases?. *Basic Clin. Pharmacol. Toxicol.* **129**(3), 161–172 (2021).
22. Pahlavani, M., Kalupahana, N. S., Ramalingam, L. & Moustaid-Moussa, N. Regulation and functions of the renin–angiotensin system in white and brown adipose tissue. *Compr. Physiol.* **7**(4), 1137–1150 (2017).
23. Chen, G. et al. Sodium butyrate inhibits inflammation and maintains epithelium barrier integrity in a TNBS-induced inflammatory bowel disease mice model. *EBioMedicine* **30**, 317–325 (2018).
24. Shi, Y. et al. Activation of the renin–angiotensin system promotes colitis development. *Sci. Rep.* **6**(1), 27552 (2016).
25. Cooper, H. S., Murthy, S. N., Shah, R. S. & Sedergran, D. J. Clinicopathologic study of dextran sulfate sodium experimental murine colitis. *Lab. Invest.: A J. Tech. Methods Pathol.* **69**(2), 238–249 (1993).
26. Axelsson, M. & Gentili, F. A single-step method for rapid extraction of total lipids from green microalgae. *PLoS ONE* **9**(2), e89643 (2014).
27. Appleyard, C. B. & Wallace, J. L. Reactivation of hapten-induced colitis and its prevention by anti-inflammatory drugs. *Am. J. Physiol. Gastrointest. Liver Physiol.* **269**(1), G119–G125 (1995).
28. Garg, M. et al. Imbalance of the renin–angiotensin system may contribute to inflammation and fibrosis in IBD: A novel therapeutic target?. *Gut* **69**(5), 841–851 (2020).
29. Mehandru, S. & Colombel, J. F. The intestinal barrier, an arbitrator turned provocateur in IBD. *Nat. Rev. Gastroenterol. Hepatol.* **18**(2), 83–84 (2020).
30. Rohr, M. W., Narasimhulu, C. A., Rudeski-Rohr, T. A. & Parthasarathy, S. Negative effects of a high-fat diet on intestinal permeability: A review. *Adv. Nutr.* **11**(1), 77–91 (2019).
31. Ellulu, M. S., Patimah, I., Khazaai, H., Rahmat, A. & Abed, Y. Obesity and inflammation: The linking mechanism and the complications. *Arch. Med. Sci.* **13**(4), 851–863 (2017).
32. Kwaifa, I. K., Bahari, H., Yong, Y. K. & Noor, S. M. Endothelial dysfunction in obesity-induced inflammation: Molecular mechanisms and clinical implications. *Biomolecules* **10**(2), 291 (2020).
33. Chelakkot, C., Ghim, J. & Ryu, S. H. Mechanisms regulating intestinal barrier integrity and its pathological implications. *Exp. Mol. Med.* **50**(8), 1–9 (2018).
34. Lee, S. H. Intestinal permeability regulation by tight junction: Implication on inflammatory bowel diseases. *Intest. Res.* **13**(1), 11–18 (2015).
35. Li, X. et al. Somatostatin regulates tight junction proteins expression in colitis mice. *Int. J. Clin. Exp. Pathol.* **7**(5), 2153 (2014).
36. Llewellyn, S. R. et al. Interactions between diet and the intestinal microbiota alter intestinal permeability and colitis severity in mice. *Gastroenterology* **154**(4), 1037–1046 (2017).
37. Engeli, S. et al. The adipose-tissue renin–angiotensin–aldosterone system: Role in the metabolic syndrome?. *Int. J. Biochem. Cell Biol.* **35**(6), 807–825 (2003).
38. Rahmouni, K., Mark, A. L., Haynes, W. G. & Sigmund, C. D. Adipose depot-specific modulation of angiotensinogen gene expression in diet-induced obesity. *Am. J. Physiol.-Endocrinol. Metab.* **286**(6), E891–E895 (2004).
39. Rasha, F. et al. Mechanisms linking the renin–angiotensin system, obesity, and breast cancer. *Endocr.-Relat. Cancer* **26**(12), R653–R672 (2019).
40. Weisinger, R. S., Begg, D. P., Chen, N. & Jois, M. The problem of obesity: Is there a role for antagonists of the renin–angiotensin system? **16** Suppl 1, 359–367 (2007).
41. Lee, C. et al. Enalapril inhibits nuclear factor- $\kappa$ B signaling in intestinal epithelial cells and peritoneal macrophages and attenuates experimental colitis in mice. *Life Sci.* **95**(1), 29–39 (2014).

## Author contributions

All authors contributed to the study conception and design. XL conceived and designed research; MMP and QX performed experiments; LJH and YYB analyzed data and prepared figures; XL and YBT interpreted results of experiments and drafted manuscript; all authors approved final version of manuscript.

## Funding

We gratefully acknowledge the financial support received from the Medical Science and Technology Project of Zhejiang Province (Grant Number: 2024KY670, 2025KY630).

## Declarations

## Competing interests

The authors declare no competing interests.

## Additional information

**Supplementary Information** The online version contains supplementary material available at <https://doi.org/10.1038/s41598-025-19294-y>.

**Correspondence** and requests for materials should be addressed to X.L. or Y.T.

**Reprints and permissions information** is available at [www.nature.com/reprints](http://www.nature.com/reprints).

**Publisher's note** Springer Nature remains neutral with regard to jurisdictional claims in published maps and institutional affiliations.

**Open Access** This article is licensed under a Creative Commons Attribution-NonCommercial-NoDerivatives 4.0 International License, which permits any non-commercial use, sharing, distribution and reproduction in any medium or format, as long as you give appropriate credit to the original author(s) and the source, provide a link to the Creative Commons licence, and indicate if you modified the licensed material. You do not have permission under this licence to share adapted material derived from this article or parts of it. The images or other third party material in this article are included in the article's Creative Commons licence, unless indicated otherwise in a credit line to the material. If material is not included in the article's Creative Commons licence and your intended use is not permitted by statutory regulation or exceeds the permitted use, you will need to obtain permission directly from the copyright holder. To view a copy of this licence, visit <http://creativecommons.org/licenses/by-nc-nd/4.0/>.

© The Author(s) 2025